

We are IntechOpen, the world's leading publisher of Open Access books Built by scientists, for scientists

6,900

Open access books available

185,000

International authors and editors

200M

Downloads

Our authors are among the

154

Countries delivered to

TOP 1%

most cited scientists

12.2%

Contributors from top 500 universities



WEB OF SCIENCE™

Selection of our books indexed in the Book Citation Index
in Web of Science™ Core Collection (BKCI)

Interested in publishing with us?
Contact book.department@intechopen.com

Numbers displayed above are based on latest data collected.
For more information visit www.intechopen.com



Axisymmetric Indentation Response of Functionally Graded Material Coating

Tie-Jun Liu

Abstract

In this chapter, the indentation response of the functionally graded material (FGM) coating is considered due to the contact between the coating and axisymmetric indenter. The mechanical properties of FGM coating is assumed to vary along the thickness direction. Three kinds of models are applied to simulate the variation of elastic parameter in the FGM coating based on the cylindrical coordinate system. The axisymmetric frictionless and partial slip contact problems are reduced to a set of Cauchy singular integral equations that can be numerically calculated by using the Hankel integral transform technique and the transfer matrix method. The effect of gradient of coating on the distribution of contact stress is presented. The present investigation will provide the guidance for the indentation experiment of coating.

Keywords: functionally graded material, coating, indentation, axisymmetric contact

1. Introduction

Functionally graded material (FGM) [1] which is new kind of nonhomogeneous composite material has many predominant properties, so it has been widely used in many fields. In recent years, many researchers have conducted the experiment to prove that FGM used as coatings can resist the contact deformation and reduce the interface damage [2], so it is very important to study the indentation response of FGM coating. Because FGM are composites whose material properties vary gradually along a coordinate axis, the governing equations which represent the mechanical behaviors of the materials are very difficult to solve. Researchers usually describe the properties of FGM according to some specific functional forms such as exponential functions and power law functions of elastic modulus [3, 4]. By assuming the elastic modulus of FGM varying as exponential function form, Guler and Erdogan [5, 6] studied the two-dimensional contact problem of functionally graded coatings. Liu et al. [7, 8] investigated the axisymmetric contact problem of FGM coating and interfacial layer with exponentially varying modulus by using the singular integral equation. The axisymmetric problems for a nonhomogeneous elastic layer in which the shear modulus follows the power law function are taken into account by Jeon et al. [9]. Because solving the controlling equations of FGM is difficult, the contact problem of FGM is limited to assume the elastic modulus

varying as some specific functional forms. To eliminate this disadvantage, Ke and Wang [10, 11] applied the linear multilayered (LML) model to simulate the FGM with arbitrarily varying elastic parameter. Based on the model, some two-dimensional contact problems are studied. The axisymmetric contact problem of FGM coating with arbitrary spatial variation of material properties is considered by making use of the extended linear multilayered model [12, 13]. Recently, a piecewise exponential multilayered (PWEML) model [14] is presented to solve the frictionless contact problem of FGM with the shear modulus of the coating varying in the power law form. Subsequently, Liu and Li [15] applied the model to solve the two-dimensional adhesive contact problem.

When two bodies are brought together under the applied force, contact occurs at interface. Hertz [16] first considers the frictionless contact problem between elastic bodies. Researchers obtained the classical solution to the indentation problem under the flat, cylindrical, and cone punch based on Hertz's theory [17]. The contact tractions and displacement field can be given to characterize the mechanical properties of various materials. Liu et al. [7, 12, 14] solved the axisymmetric frictionless contact problem for FGM coating by using the singular integral equation. They discussed the effect of the gradient of FGM coating on the indentation response. Because the materials of the two contact solids are dissimilar, the slip will take place at the contact surface. If slip is opposed by friction, the contact region is divided into two parts: the stick region and the slip region. Spence [18] gives the contact stress fields in homogeneous materials by assuming a self-similarity at each stage of finite friction contact when the normal load monotonically increases. Ke and Wang [19] solved the two-dimensional contact problem with finite friction for FGM coating. Liu et al. [13] considered the axisymmetric partial slip contact problem of a graded coating. When the coefficient of friction is sufficiently large, slip might be prevented entirely. The self-similar solution to nonslip contact problems with incremental loading was considered by Spence [20]. Goodman [21] investigated the axisymmetric contact problem with full stick when elastically dissimilar spheres are pressed together. Mossakowski [22] studied contact with adhesion for the elastic bodies under condition of adhesion. Norwell et al. [23] adopt an iteration method to solve the coupled equations which can describe the partial slip contact problem.

In this chapter, the axisymmetric frictionless and partial slip contact problems for FGM coating are considered. The basic formulation for nonhomogeneous material layer with elastic parameter varying along the thickness direction is given in Section 2. Based on the basic formulations for nonhomogeneous layer, three types of computational model for FGM coating are introduced in Section 3 for axisymmetric contact problem. The displacement and stress components in the transform domain are gained by using the Hankel transform technology and transfer matrix method. In Section 4, we will investigate the solution for the axisymmetric frictionless and partial slip contact problems. The indentation response of FGM coating under frictionless and frictional condition will be discussed in Section 5. Finally, we will depict some conclusions on the axisymmetric indentation response of FGM coating.

2. Basic formulations for nonhomogeneous material layer

For the present axisymmetric problem, the strain components, stress-strain relations, and the equilibrium equations in the radial and axial directions disregarding the body forces are given by the following relations [7]:

$$\varepsilon_{rr} = \frac{\partial u}{\partial r}, \quad (1a)$$

$$\varepsilon_{\theta\theta} = \frac{u}{r}, \quad (1b)$$

$$\varepsilon_{zz} = \frac{\partial w}{\partial z}, \quad (1c)$$

$$2\varepsilon_{rz} = \frac{\partial u}{\partial z} + \frac{\partial w}{\partial r}. \quad (1d)$$

$$\sigma_{rr} = (\lambda(z) + 2\mu(z)) \frac{\partial u}{\partial r} + \lambda(z) \left(\frac{u}{r} + \frac{\partial w}{\partial z} \right), \quad (2a)$$

$$\sigma_{\theta\theta} = (\lambda(z) + 2\mu(z)) \frac{u}{r} + \lambda(z) \left(\frac{\partial u}{\partial r} + \frac{\partial w}{\partial z} \right), \quad (2b)$$

$$\sigma_{zz} = (\lambda(z) + 2\mu(z)) \frac{\partial w}{\partial z} + \lambda(z) \left(\frac{\partial u}{\partial r} + \frac{u}{r} \right), \quad (2c)$$

$$\sigma_{rz} = \mu(z) \left(\frac{\partial u}{\partial z} + \frac{\partial w}{\partial r} \right). \quad (2d)$$

$$\frac{\partial \sigma_{rr}}{\partial r} + \frac{\partial \sigma_{rz}}{\partial z} + \frac{1}{r} (\sigma_{rr} - \sigma_{\theta\theta}) = 0, \quad (3a)$$

$$\frac{\partial \sigma_{rz}}{\partial r} + \frac{\partial \sigma_{zz}}{\partial z} + \frac{1}{r} \sigma_{rz} = 0. \quad (3b)$$

in which r and z are the variables of the cylindrical coordinate system; ε_{rr} , $\varepsilon_{\theta\theta}$, ε_{zz} , and ε_{rz} are the strain components; u and w are the displacement components in the radial and axial directions; σ_{rr} , $\sigma_{\theta\theta}$, σ_{zz} , and σ_{rz} are the stress components; $\lambda(z)$ and $\mu(z)$ are Lamé's constants which vary along the z -axis direction.

3. Computational models for FGM coating

The properties of nonhomogeneous material may vary arbitrarily along a certain spatial direction, which makes the solution of contact problem very difficult in mathematics. In the present work, we adopt three methods to model the axisymmetric FGM layer based on the cylindrical coordinate system. First, exponential function (EF) model [7] is used to assume the elastic modulus of the FGM layer that varies as the exponential function. Second, the linear multi-layered (LML) model [12] is applied to simulate the FGM layer with arbitrarily varying material modulus, and Poisson's ratio is chosen as 1/3. The model divided FGM layer into a series of sub-layers in which the shear modulus varies as linear function form. The shear modulus is taken to be continuous at the sub-interfaces and equal to their real values. Third, the piecewise exponential multilayered (PWEML) model [14] is employed in modeling the functionally graded material layer with arbitrary spatial variation of material properties. In this model, the functionally graded layer is cut into several sub-layers where the elastic parameter varies according to the exponential function form. Three types of computational model for FGM coating are the following.

3.1 Exponential function model

In **Figure 1(a)**, the shear modulus of the functionally graded coating can be described by

$$\mu(z) = \mu_0 e^{\alpha z} \quad (4)$$

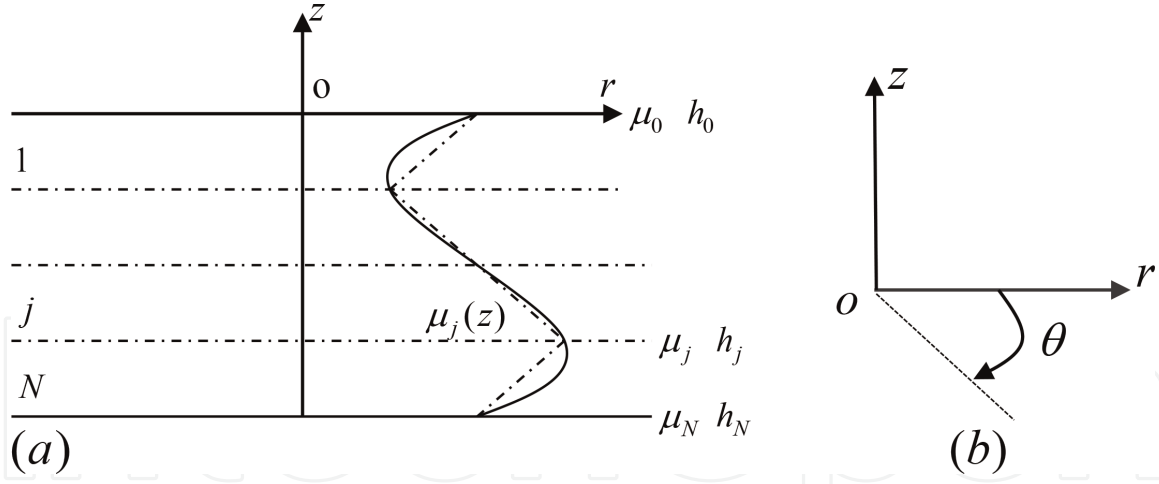


Figure 1. The linear multi-layered model for the functionally graded coating (a) and the cylindrical coordinate system (b).

where $\alpha = h_0^{-1} \log(\mu_0/\mu^*)$ is a constant characterizing the material inhomogeneity with μ_0 being the value of $\mu(z)$ at the surface, i.e., $\mu_0 = \mu(h_0)$. μ_0 and μ^* are related by

$$\mu_0 = \mu^* e^{\alpha h_0} \quad (5)$$

Substituting Eqs. (2) and (5) into Eq. (3), we obtain

$$(k+1) \left\{ \frac{\partial^2 u}{\partial r^2} + \frac{1}{r} \frac{\partial u}{\partial r} - \frac{1}{r^2} u + \frac{\partial^2 w}{\partial r \partial z} \right\} + (k-1) \alpha \left(\frac{\partial u}{\partial z} + \frac{\partial w}{\partial r} \right) + (k-1) \left\{ \frac{\partial^2 u}{\partial z^2} - \frac{\partial^2 w}{\partial r \partial z} \right\} = 0, \quad (6a)$$

$$(k+1) \left\{ \frac{\partial^2 u}{\partial r \partial z} + \frac{1}{r} \frac{\partial u}{\partial z} + \frac{\partial^2 w}{\partial z^2} \right\} - (k-1) \left(\frac{\partial^2 u}{\partial r \partial z} - \frac{\partial^2 w}{\partial r^2} \right) - \frac{(k-1)}{r} \left\{ \frac{\partial u}{\partial z} - \frac{\partial w}{\partial r} \right\} + (3-k) \alpha \left(\frac{\partial u}{\partial r} + \frac{u}{r} \right) + (k+1) \alpha \frac{\partial w}{\partial z} = 0 \quad (6b)$$

where $k = 3 - 4\nu$ and ν is Poisson's ratio.

In order to solve Eq. (6), we use the technique of Hankel integral transform. The Hankel transform and its inversion are defined as

$$\langle \tilde{\omega}(s, z) \rangle_p = \int_0^\infty \omega(s, z) r J_p(sr) dr, \quad (7a)$$

$$\omega_p(r, z) = \int_0^\infty \langle \tilde{\omega}(s, z) \rangle_p s J_p(sr) ds \quad (7b)$$

where the bar \sim indicates Hankel transform; $\langle \rangle_p$ is the p th-order Hankel transform; and J_p is the p th-order Bessel function of the first kind.

By using the Hankel transform and defining $D = d/dz$, Eq. (6) can be expressed as

$$\{(k-1)D^2 + \alpha(k-1)D - (k+1)s^2\} \langle \tilde{u} \rangle_1 - \{2sD + \alpha s(k-1)\} \langle \tilde{w} \rangle_0 = 0, \quad (8a)$$

$$\{2sD + \alpha(3 - k)s\}\langle\tilde{u}\rangle_1 + \{(k + 1)D^2 + \alpha(k + 1)D - (k - 1)s^2\}\langle\tilde{w}\rangle_0 = 0, \quad (8b)$$

The solution of the differential Eqs. (8) is given by [7]

$$\langle\tilde{u}\rangle_1 = A_3(s)e^{m_1z} + A_4(s)e^{m_2z} + A_5(s)e^{m_3z} + A_6(s)e^{m_4z} \quad (9a)$$

$$\langle\tilde{w}\rangle_0 = A_3(s)a_1e^{m_1z} + A_4(s)a_2e^{m_2z} + A_5(s)a_3e^{m_3z} + A_6(s)a_4e^{m_4z} \quad (9b)$$

where

$$a_i = -\frac{2sm_i + s\alpha(3 - k)}{(k + 1)m_i^2 + \alpha(k + 1)m_i - (k - 1)s^2}, (i = 1, \dots, 4)$$

and

$$\begin{aligned} m_1 &= -\frac{\alpha}{2} + \frac{1}{2} \left\{ \alpha^2 + 4s^2 + i4\sqrt{\frac{3-k}{k+1}}\alpha s \right\}^{1/2}, \\ m_2 &= -\frac{\alpha}{2} - \frac{1}{2} \left\{ \alpha^2 + 4s^2 + i4\sqrt{\frac{3-k}{k+1}}\alpha s \right\}^{1/2}, \\ m_3 &= -\frac{\alpha}{2} + \frac{1}{2} \left\{ \alpha^2 + 4s^2 - i4\sqrt{\frac{3-k}{k+1}}\alpha s \right\}^{1/2}, \\ m_4 &= -\frac{\alpha}{2} - \frac{1}{2} \left\{ \alpha^2 + 4s^2 - i4\sqrt{\frac{3-k}{k+1}}\alpha s \right\}^{1/2}. \end{aligned}$$

According to Hooke's law and strain-displacement relations, stress components may be expressed as

$$\frac{\kappa - 1}{\mu(z)} \langle\tilde{\sigma}_{zz}\rangle_0 = \sum_{i=1}^4 \{(\kappa + 1)m_i a_i + (3 - k)s\} A_{i+2} e^{m_i z} \quad (10a)$$

$$\frac{1}{\mu(z)} \langle\tilde{\sigma}_{rz}\rangle_1 = \sum_{i=1}^4 \{m_i - a_i s\} A_{i+2} e^{m_i z} \quad (10b)$$

For a homogeneous layer without the gradient, the gradient index α in Eqs. (9) and (10) equals to 0.

3.2 Linear multi-layered model

Consider the linear multi-layered model shown in **Figure 1**. The shear modulus of the functionally graded coating can be described by an arbitrary continuous function of z , $\mu(z)$, with boundary values $\mu(h_0) = \mu_0$. Poisson's ratio ν is taken as 1/3. The linear multilayered model divides functionally graded coating into N sub-layers. The shear modulus $\mu(z)$ in each sub-layer is assumed to take the following form:

$$\mu(z) \approx \mu_j(z) = c_j(1 + z/b_j) = c_j \left(\frac{z^*}{b_j} \right), h_j \leq z \leq h_{j-1}, j = 1, 2, \dots, N \quad (11)$$

where $z^* = z + b$ and μ_j is equal to the real value of the shear modulus at the sub-interfaces, $z = h_j$, i.e., $\mu_j(h_j) = \mu(h_j)$, which lead to

$$b_j = \frac{\mu_{j-1}h_j - \mu_j h_{j-1}}{\mu_j - \mu_{j-1}}, \quad (12a)$$

$$c_j = \frac{\mu_j}{1 + h_j/b_j}. \quad (12b)$$

As in [12], introduces two potential functions to write the displacement components u_j and w_j in each sub-layer:

$$u_j = (z + b_j)\partial f_j/\partial r + \partial \phi_j/\partial r \quad (13a)$$

$$w_j = (z + b_j)\partial f_j/\partial z - f_j + \partial \phi_j/\partial z, \quad (h_j \leq z \leq h_{j-1}). \quad (13b)$$

By making use of Eqs. (1), (2), and (13), the equilibrium equations (3) are represented as [12].

$$\nabla^2 \phi_j + \frac{1}{z^*} \partial \phi_j/\partial z^* = 0, \quad (14a)$$

$$\nabla^2 f_j + \frac{1}{z^*} \partial f_j/\partial z^* = \frac{1}{2z^{*2}} \partial \phi_j/\partial z. \quad (14b)$$

where

$$\nabla^2 = \frac{1}{r} \partial(r\partial/\partial r)/\partial r + \partial^2/\partial z^{*2}.$$

Then the displacement and stress components given by Eqs. (13) and (2) are given by

$$u_j = z^* \partial f_j/\partial r + \partial \phi_j/\partial r, \quad (h_j \leq z \leq h_{j-1}) \quad (15a)$$

$$w_j = z^* \partial f_j/\partial z^* - f_j + \partial \phi_j/\partial z^*, \quad (h_j \leq z \leq h_{j-1}) \quad (15b)$$

$$\sigma_{rrj} = 2c_j \left(\frac{z^*}{b_j} \right) \left(z^* \partial^2 f_j/\partial r^2 + \partial^2 \phi_j/\partial r^2 - \partial f_j/\partial z^* - \frac{1}{2z^*} \partial \phi_j/\partial z^* \right), \quad (16a)$$

$$\sigma_{\theta\theta j} = 2c_j \left(\frac{z^*}{b_j} \right) \left(z^* \frac{1}{r} \partial f_j/\partial r + \frac{1}{r} \partial \phi_j/\partial r - \partial f_j/\partial z^* - \frac{1}{2z^*} \partial \phi_j/\partial z^* \right), \quad (16b)$$

$$\sigma_{zzj} = 2c_j \left(\frac{z^*}{b_j} \right) \left(z^* \partial^2 f_j/\partial r^2 + \partial^2 \phi_j/\partial z^{*2} - \partial f_j/\partial z^* - \frac{1}{2z^*} \partial \phi_j/\partial z^* \right), \quad (16c)$$

$$\sigma_{rzj} = 2c_j \left(\frac{z^*}{b_j} \right) \left(z^* \partial^2 f_j/\partial r \partial z^* + \partial^2 \phi_j/\partial r \partial z^* \right). \quad (16d)$$

Applying Hankel transformation Eqs. (7a)–(14), we obtain the solutions for displacement functions ϕ_j and f_j in each sub-layer:

$$\langle \tilde{\phi}_j \rangle_0 = A_{j1}(s)I_0(sz^*) + A_{j2}(s)K_0(sz^*), \quad (17a)$$

$$\langle \tilde{f}_j \rangle_0 = A_{j3}(s)I_0(sz^*) + A_{j4}(s)K_0(sz^*) + \frac{s}{2} \{ A_{j1}(s)I_1(sz^*) - A_{j2}(s)K_1(sz^*) \} \quad (17b)$$

where I_0 , I_1 , K_0 , and K_1 are modified Bessel functions of the 0th and 1th order.

Applying Hankel transform to Eqs. (15) and (16), we get

$$\begin{aligned}\langle \tilde{u}_{rj} \rangle_1 &= -sz * \langle \tilde{f}_j \rangle_0 - s \langle \tilde{\phi}_j \rangle_0 \\ &= \left\{ -\frac{s^2}{2} z * I_1(sz *) - sI_0(sz *) \right\} A_{j1}(s) + \left\{ \frac{s^2}{2} z * K_1(sz *) - sK_0(sz *) \right\} A_{j2}(s) \\ &\quad - sz * I_0(sz *) A_{j3}(s) - sz * K_0(sz *) A_{j4}(s)\end{aligned}\quad (18a)$$

$$\begin{aligned}\langle \tilde{w}_j \rangle_0 &= z * d\langle \tilde{f}_j \rangle_0 / dz * - \langle \tilde{f}_j \rangle_0 + d\langle \tilde{\phi}_j \rangle_0 / dz * \\ &= \frac{s^2}{2} z * I_0(sz *) A_{j1}(s) + \frac{s^2}{2} z * K_0(sz *) A_{j2}(s) + \{ z * sI_1(sz *) - I_0(sz *) \} A_{j3}(s) \\ &\quad + \{ -z * sK_1(sz *) - K_0(sz *) \} A_{j4}(s)\end{aligned}\quad (18b)$$

$$\begin{aligned}\langle \tilde{\sigma}_{zzj} \rangle_0 &= 2c_j \left(\frac{z *}{b_j} \right) \left\{ \frac{s^3}{2} z * I_1(sz *) A_{j1}(s) - \frac{s^3}{2} z * K_1(sz *) A_{j2}(s) \right. \\ &\quad \left. + (z * s^2 I_0(sz *) - 2sI_1(sz *)) A_{j3}(s) + (z * s^2 K_0(sz *) + 2sK_1(sz *)) A_{j4}(s) \right\}\end{aligned}\quad (18c)$$

$$\begin{aligned}\langle \tilde{\sigma}_{rzj} \rangle_1 &= 2c_j \left(\frac{z *}{b_j} \right) \left\{ \left(-\frac{s^3}{2} z * I_0(sz *) - \frac{s^2}{2} I_1(sz *) \right) A_{j1}(s) \right. \\ &\quad \left. + \left(-\frac{s^3}{2} z * K_0(sz *) + \frac{s^2}{2} K_1(sz *) \right) A_{j2}(s) - s^2 z * I_1(sz *) A_{j3}(s) + s^2 z * K_1(sz *) A_{j4}(s) \right\}\end{aligned}\quad (18d)$$

3.3 Piece wise exponential multi-layered model

Piece wise exponential multi-layered model divides functionally graded coatings into N sub-layers as shown in **Figure 2**. The shear modulus $\mu(z)$ in each sub-layer is assumed to vary as an exponential function form:

$$\mu(z) \approx \mu_j(z) = a_j e^{b_j z}, h_j \leq z \leq h_{j-1}, j = 1, 2, \dots, N \quad (19a)$$

$$\mu(h_j) = \mu_j(h_j), \quad (19b)$$

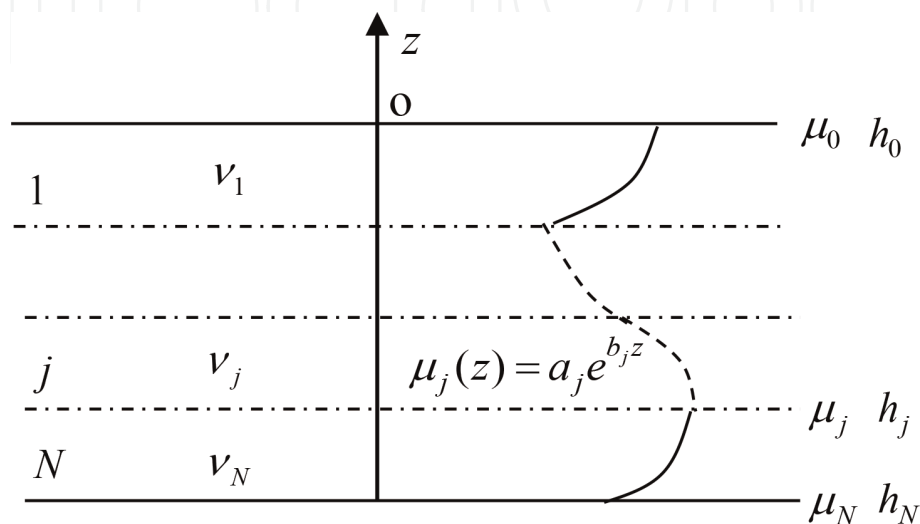


Figure 2.
Piece wise exponential multi-layered model for the graded coating.

in which:

$$a_j = \mu(h_j) e^{-\ln[\mu(h_{j+1})/\mu(h_j)]h_j/(h_{j+1}-h_j)}, b_j = \ln[\mu(h_{j+1})/\mu(h_j)]/(h_{j+1}-h_j)$$

and h_j is the z coordinate at the end of layer j . Poisson's ratio in each sub-layer is assumed to be a constant ν_j .

In each sub-layer ($j = 1, 2, \dots, N$), the equilibrium equations are represented as [14]

$$(k_j + 1) \left\{ \frac{\partial^2 u_j}{\partial r^2} + \frac{1}{r} \frac{\partial u_j}{\partial r} - \frac{1}{r^2} u_j + \frac{\partial^2 w_j}{\partial r \partial z} \right\} + (k_j - 1) b_j \left(\frac{\partial u_j}{\partial z} + \frac{\partial w_j}{\partial r} \right) + (k_j - 1) \left\{ \frac{\partial^2 u_j}{\partial z^2} - \frac{\partial^2 w_j}{\partial r \partial z} \right\} = 0, \quad (20a)$$

$$(k_j + 1) \left\{ \frac{\partial^2 u_j}{\partial r \partial z} + \frac{1}{r} \frac{\partial u_j}{\partial z} + \frac{\partial^2 w_j}{\partial z^2} \right\} - (k_j - 1) b_j \left(\frac{\partial^2 u_j}{\partial r \partial z} - \frac{\partial^2 w_j}{\partial r^2} \right) - \frac{(k_j - 1)}{r} \left\{ \frac{\partial u_j}{\partial z} - \frac{\partial w_j}{\partial r} \right\} + (3 - k_j) b_j \left(\frac{\partial u_j}{\partial r} + \frac{u_j}{r} \right) + (k_j + 1) b_j \frac{\partial w_j}{\partial z} = 0 \quad (20b)$$

where u_j and w_j are the displacement components in the radial and z axial directions in layer j and $k_j = 3 - 4\nu_j$.

The solution of differential equations (20) may be expressed as [7]

$$\langle \tilde{u}_j(s, z) \rangle_1 = A_{j1}(s) e^{m_{j1}z} + A_{j2}(s) e^{m_{j2}z} + A_{j3}(s) e^{m_{j3}z} + A_{j4}(s) e^{m_{j4}z} \quad (21a)$$

$$\langle \tilde{w}_j(s, z) \rangle_0 = A_{j1}(s) c_{j1} e^{m_{j1}z} + A_{j2}(s) c_{j2} e^{m_{j2}z} + A_{j3}(s) c_{j3} e^{m_{j3}z} + A_{j4}(s) c_{j4} e^{m_{j4}z} \quad (21b)$$

where A_{j1} – A_{j4} are unknown constants to be solved in layer j .

$$c_{ji} = -\frac{2sm_{ji} + sb_j(3 - k_j)}{(k_j + 1)m_{ji}^2 + b_j(k + 1)m_{ji} - (k_j - 1)s^2}, \quad (i = 1, 2, 3, 4)$$

$$m_{j1} = -\frac{b_j}{2} + \frac{1}{2} \left\{ b_j^2 + 4s^2 + i4\sqrt{\frac{3 - k_j}{k_j + 1}} b_j s \right\}^{1/2},$$

$$m_{j2} = -\frac{b_j}{2} - \frac{1}{2} \left\{ b_j^2 + 4s^2 + i4\sqrt{\frac{3 - k_j}{k_j + 1}} b_j s \right\}^{1/2},$$

$$m_{j3} = -\frac{b_j}{2} + \frac{1}{2} \left\{ b_j^2 + 4s^2 - i4\sqrt{\frac{3 - k_j}{k_j + 1}} b_j s \right\}^{1/2},$$

$$m_{j4} = -\frac{b_j}{2} - \frac{1}{2} \left\{ b_j^2 + 4s^2 - i4\sqrt{\frac{3 - k_j}{k_j + 1}} b_j s \right\}^{1/2}.$$

According to Hooke's law and strain-displacement relations, stress components may be expressed as

$$\frac{k_j - 1}{\mu_j(z)} \langle \tilde{\sigma}_{zzj}(s, z) \rangle_0 = \sum_{i=1}^4 \{ (k_j + 1)m_{ji}c_{ji} + (3 - k_j)s \} A_{ji} e^{m_{ji}z} \quad (22a)$$

$$\frac{1}{\mu_j(z)} \langle \tilde{\sigma}_{rzj}(s, z) \rangle_1 = \sum_{i=1}^4 \{m_{ji} - c_{ji}s\} A_{ji} e^{m_{ji}z} \quad (22b)$$

4. Solution for the axisymmetric frictionless and partial slip contact problem

In this section, we will solve axisymmetric contact and fretting problem for the functionally graded coating bonded to the homogeneous half-space under the spherical indenter. A functionally graded coated half-space subjected to normal and radical distributed external loads is shown in **Figure 3**. The stresses and displacements are continuous at the interfaces, $z = 0$, which state.

$$u_2(r, 0) - u_1(r, 0) = 0, \quad (23a)$$

$$w_2(r, 0) - w_1(r, 0) = 0, \quad (23b)$$

$$\sigma_{2zz}(r, 0) - \sigma_{1zz}(r, 0) = 0, \quad (23c)$$

$$\sigma_{2rz}(r, 0) - \sigma_{1rz}(r, 0) = 0. \quad (23d)$$

And along the coating surface, $z = h_0$, we have

$$\sigma_{1zz}(r, h_0) = p(r) \quad (0 \leq r \leq a), \quad (24a)$$

$$\sigma_{1zz}(r, h_0) = 0 \quad (a < r < \infty), \quad (24b)$$

$$\sigma_{1rz}(r, h_0) = q(r) \quad (0 \leq r \leq a), \quad (24c)$$

$$\sigma_{1rz}(r, h_0) = 0 \quad (a < r < \infty) \quad (24d)$$

in which $i = 1$ refers to the graded coating and $i = 2$ refers to the homogeneous half-space. $p(r)$ and $q(r)$ are normal contact tractions and shear stress, respectively.

By using the Hankel integral transform technique and transfer matrix method, the surface displacement components can be expressed as

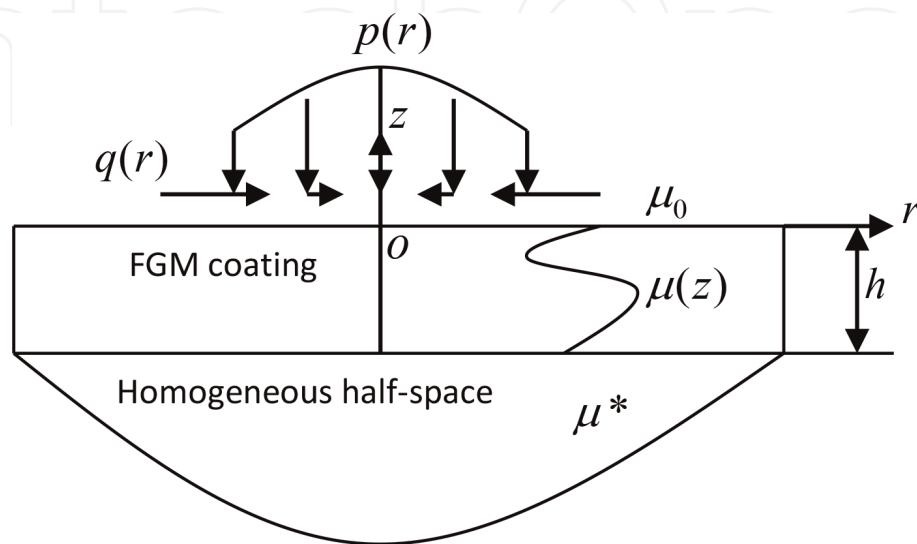


Figure 3.
 A functionally graded coated half-space subjected to normal and radical distributed external loads.

$$w_0(r) = \int_0^a p(t)t \int_0^\infty sM_{11}(s, h_0)J_0(st)J_0(sr)dsdt + \int_0^a q(t)t \int_0^\infty sM_{12}(s, h_0)J_1(st)J_0(sr)dsdt \quad (25a)$$

$$u_0(r) = \int_0^a p(t)t \int_0^\infty sM_{21}(s, h_0)J_0(st)J_1(sr)dsdt + \int_0^a q(t)t \int_0^\infty sM_{22}(s, h_0)J_1(st)J_1(sr)dsdt \quad (25b)$$

where $J_0(\cdot)$ and $J_1(\cdot)$ are Bessel functions and

$$\begin{bmatrix} M_{11}(s, h_0) & M_{12}(s, h_0) \\ M_{21}(s, h_0) & M_{22}(s, h_0) \end{bmatrix} = \frac{1}{2\mu_0} \mathbf{B}_3 \mathbf{M},$$

$$\mathbf{M} = [T_1(h_0 + b_1)] [\bar{\mathbf{V}}_1] \{ [B][T_1(h_0 + b_1)] [\bar{\mathbf{V}}_1] \}^{-1},$$

$$\mathbf{B}_3 = \begin{bmatrix} 0 & 1 & 0 & 0 \\ 1 & 0 & 0 & 0 \end{bmatrix}, \mathbf{C} = \begin{bmatrix} 1 & 0 \\ 0 & 1 \end{bmatrix}.$$

where $M_{ij}(s, h_0)$ is the kernel function (see Ref. [13]).

Considering the asymptotic behavior of Bessel functions for large arguments [13], one may prove

$$\lim_{s \rightarrow \infty} \begin{bmatrix} sM_{11}(s, h_0) & sM_{12}(s, h_0) \\ sM_{21}(s, h_0) & sM_{22}(s, h_0) \end{bmatrix} = \begin{bmatrix} \alpha_{11} & \alpha_{12} \\ \alpha_{21} & \alpha_{22} \end{bmatrix} = \begin{bmatrix} \frac{1-v}{\mu_0} & \frac{1-2v}{2\mu_0} \\ \frac{1-2v}{2\mu_0} & \frac{1-v}{\mu_0} \end{bmatrix}. \quad (26)$$

Differentiation of Eq. (5) with respect to r and extension of the definition of the unknown functions, $p(r)$ and $q(r)$, into the range $-a \leq r \leq 0$ yields.

$$m_1(r) = \frac{1}{2} \int_{-a}^a \{p(t)|t|I_{11}(r, t) + q(t)|t|I_{12}(r, t)\}dt + \frac{\alpha_1}{\pi} \int_{-a}^a \frac{p(t)}{t-r}dt + \frac{\alpha_1}{\pi} \int_{-a}^a p(t)H_1(r, t)dt - \alpha_2 q(r) \quad (27a)$$

$$m_2(r) = \frac{1}{2} \int_{-a}^a \{q(t)|t|I_{22}(r, t) + p(t)|t|I_{21}(r, t)\}dt + \frac{\alpha_1}{\pi} \int_{-a}^a \frac{q(t)}{t-r}dt + \frac{\alpha_1}{\pi} \int_{-a}^a q(t)H_2(r, t)dt + \alpha_2 p(r) \quad (27b)$$

where

$$m_1(r) = \frac{\partial u_{z0}(r, h_0)}{\partial r}, m_2(r) = \frac{1}{r} \frac{\partial ru_{r0}(r, h_0)}{\partial r}, H_i(r, t) = (h_i(r, t) - 1)/(t - r),$$

$$I_{ij}(r,t) = (-1)^i \int_0^\infty (sM_{ij}(s,h_0) - \alpha_{ij}) sJ_{2-i}(sr)J_{j-1}(st)ds, (i = 1, 2, j = 1, 2),$$

$$h_1(r,t) = \begin{cases} |t/r|E(t/r), & (|t| < |r|) \\ (t^2/r^2)E(r/t) - \{(t^2 - r^2)/r^2\}K(r/t), & (|t| > |r|) \end{cases},$$

$$h_2(r,t) = \begin{cases} \{(t^2 - r^2)/|tr|\}K(t/r) + (r/t)E(t/r), & (|t| < |r|) \\ E(r/t), & (|t| > |r|) \end{cases},$$

with $K(.)$ and $E(.)$ being, respectively, the complete elliptic integrals of the first and second kinds.
 The system of the singular integrals, Eqs. (27a) and (27b), must be solved subjected to the following condition:

$$P = \pi \int_{-a}^a p(t)tdt \tag{28}$$

4.1 Frictionless contact problem of FGM coating

In this section, the axisymmetric frictionless contact problem between FGM coatings and a rigid spherical punch is studied. As shown in **Figure 4**, an applied force P is acted on the rigid spherical punch along the z -direction to form an indent depth δ_0 and a circular contact region with a radius a . The displacement boundary condition in the contact region is expressed as

$$w(r,h_0) = \delta_0 - r^2/2R \ (0 \leq r \leq a) \tag{29}$$

Because the frictionless contact is considered, the shear traction $q(r)$ is zero, and the controlling equation is

$$m_1(r) = \frac{1}{2} \int_{-a}^a p(t)|t|I_{11}(r,t)dt + \frac{\alpha_1}{\pi} \int_{-a}^a \frac{p(t)}{t-r}dt + \frac{\alpha_1}{\pi} \int_{-a}^a p(t)H_1(r,t)dt \tag{30}$$

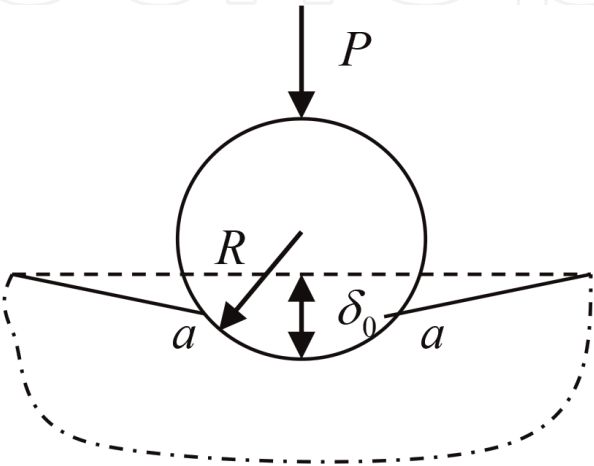


Figure 4.
 FGM coating indented by a spherical indenter.

The Gauss-Chebyshev integration formula [24] is applied to solve Eqs. (28) and (30) with the consideration of Eq. (29).

4.2 Partial slip contact problem with finite friction for FGM coating

Consider the axisymmetric partial slip contact problem as shown in **Figure 5**. The normal surface displacement, u_{z0} , along the coating interface, $z = h_0$, is given by

$$u_{z0}(r) = \delta_0 - r^2/2R \quad (31)$$

The inner stick region, $r \leq b$, and outer slip annulus, $b \leq r \leq a$, are shown in **Figure 5**. According to Spence's work [18], the radial displacement along the coating interface in the stick region may be expressed as

$$u_{r0}(r) = Cr^2, (r \leq b) \quad (32)$$

where C denotes the slope of the relative radial displacement gradient and is an unknown constant. The Coulomb friction law is applied to describe the slip behavior in the slip region. Then, the radial shear traction in the contact region is represented as

$$q(r) = q^*(r) - fp(b)\frac{r}{b}, (r \leq b), \quad (33a)$$

$$q(r) = -fp(r), (b \leq r \leq a). \quad (33b)$$

where f denotes the friction coefficient.

Finally, the partial slip contact problem with consideration of the boundary conditions (31), (32), and (33) can be expressed according to the singular integral equations:

$$\begin{aligned} & -\alpha_2 q(r) + \frac{\alpha_1}{\pi} \int_{-a}^a \frac{p(t)}{t-r} dt + \frac{\alpha_1}{\pi} \int_{-a}^a p(t) H_1(r, t) dt + \frac{1}{2} \int_{-a}^a \{p(t)|t|I_{11}(r, t) + q(t)|t|I_{12}(r, t)\} dt \\ & = -r/R, \end{aligned} \quad (34a)$$

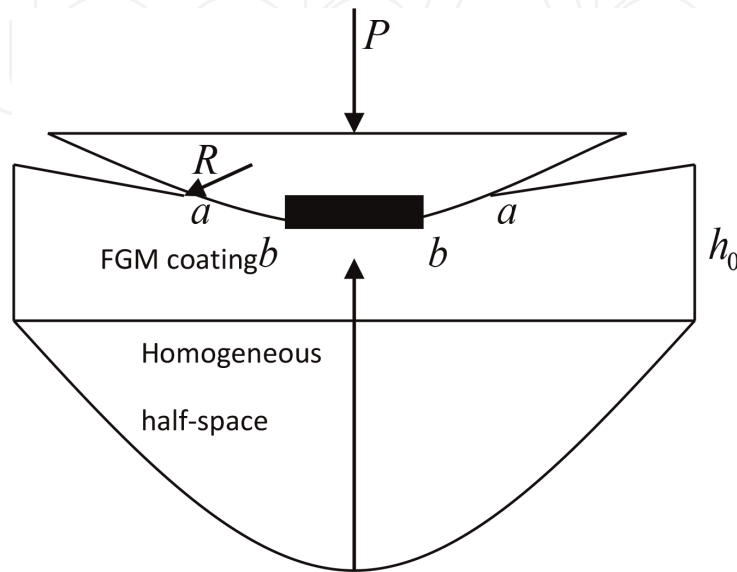


Figure 5.
A functionally graded coated half-space indented by a spherical indenter.

$$\begin{aligned} \alpha_2 p(r) + \frac{\alpha_1}{\pi} \int_{-a}^a \frac{q(t)}{t-r} dt + \frac{\alpha_1}{\pi} \int_{-a}^a q(t) H_2(r, t) dt + \frac{1}{2} \int_{-a}^a \{q(t)|t|I_{22}(r, t) + p(t)|t|I_{21}(r, t)\} dt \\ = 3C|r| \end{aligned} \quad (34b)$$

The Goodman approximate method (uncoupled solution) [21] and the iteration method (coupled solution) [13] are used to solve coupled singular integral equation (34).

5. Indentation response of FGM coating under a spherical indenter

The indentation response of FGM coating under frictionless and frictional condition will be presented in this section.

Firstly, the effects of the stiffness ratio μ_0/μ^* on the distributions of the contact pressure and the relation between indentation and applied force are investigated for the frictionless contact problem. The exponential function model is applied to obtain the results shown in **Figures 6** and **7** [7]. The distribution of the dimensionless contact pressure $p(r)$ (a) and radial stress $\sigma_{rr}(r)$ (b) on the surface of FGM coating indented by a rigid spherical indenter for various stiffness ratio μ_0/μ^* when $R/h_0 = 10$ and $a/h_0 = 0.2$ is shown in **Figure 6**. With the increase of μ_0/μ^* , the contact pressure $p(r)$ decreases. It can be observed that the tensile spike in the distribution of $\sigma_{rr}(r)$ as $r \rightarrow a$ has clearly some implications regarding the initiation and subcritical growth of surface cracks. **Figure 7** presented the relation of P vs. a and P vs. δ_0 . With the decrease of μ_0/μ^* , the larger applied normal load is needed to create the same contact region (a) and the same maximum indentation depth δ_0 (b). The results give an indentation testing method to measure the stiffness of the coating surface and the gradient of the coating.

Secondly, the linear multi-layered model is used to model the shear modulus of the coating varying in the following power law form:

$$\mu(z) = \mu^* + (\mu_0 - \mu^*)(z/h_0)^n, \quad (35)$$

where n is a gradient index characterizing the gradual variation of the shear modulus. In the following calculation, the LML model divided the FGM coating into

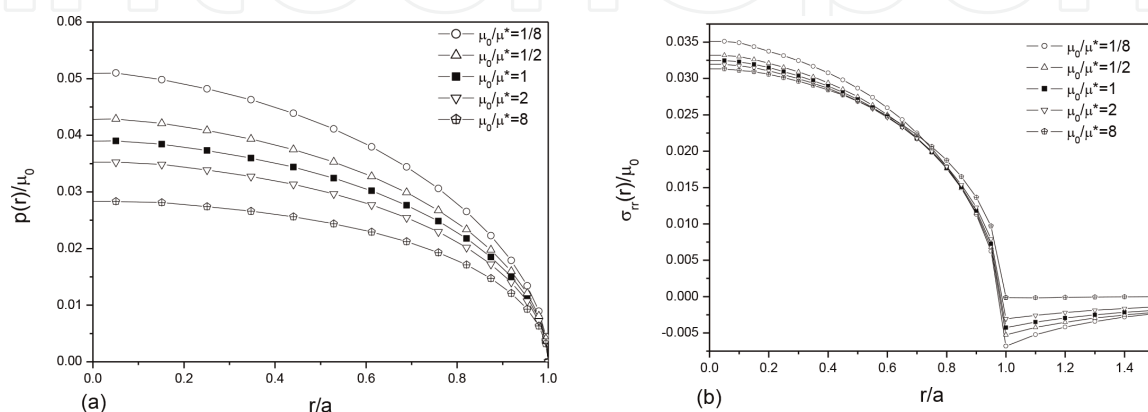


Figure 6. Distribution of the dimensionless contact pressure $p(r)$ (a) and radial stress $\sigma_{rr}(r)$ (b) on the surface of the graded coating loaded by a rigid spherical indenter for some selected values of the stiffness ratio μ_0/μ^* with $R/h_0 = 10$ and $a/h_0 = 0.2$.

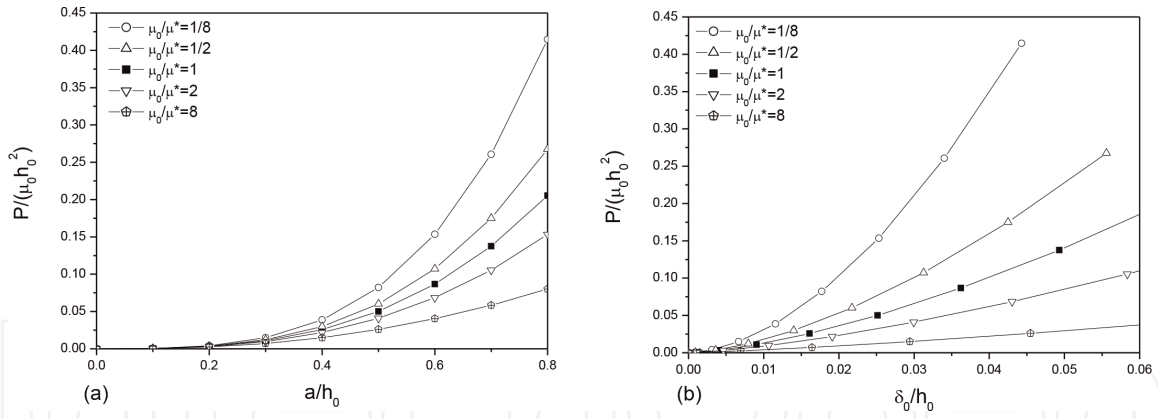


Figure 7. Relations of P vs. a (a) and P vs. δ_0 (b) for some selected values of the stiffness ratio μ_0/μ^* with $R/h_0 = 10$.

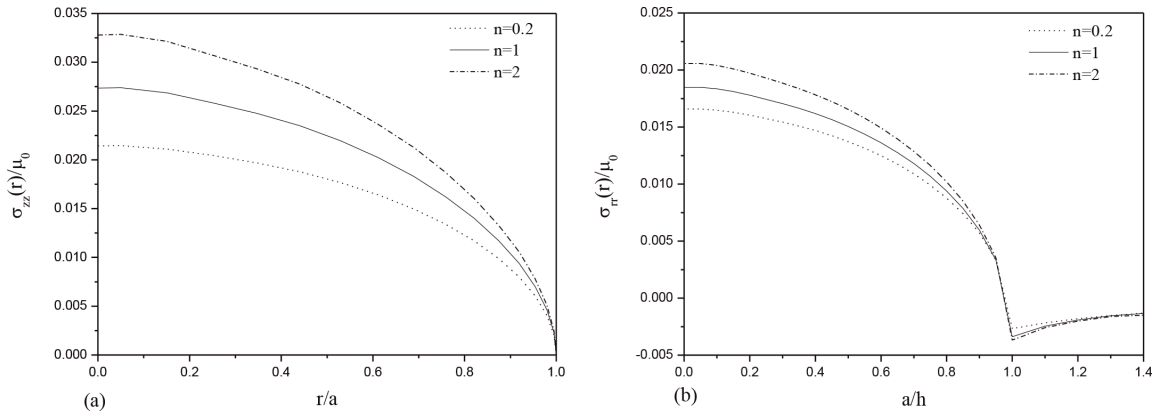


Figure 8. Distribution of the dimensionless contact pressure $\sigma_{zz}(r)$ (a) and radial stress $\sigma_{rr}(r)$ (b) for some selected values n with $a/h = 0.1$ and $R/h_0 = 10$.

six sub-layers. The axisymmetric indentation response for the frictionless contact under the spherical indenter is considered.

Figure 8 shows the distributions of the contact pressure for some selected values of n with $\mu_0/\mu^* = 1/8$ and $a/h_0 = 0.1$ [12]. With the increase of n , the contact pressure obviously increases. This behavior shows that the contact traction can be improved by adjusting the gradient of the coating when the stiffness of the coating surface keeps unchanged. When the FGM coating is indented by a conical indenter, the relations of P vs. a (a) and P vs. δ_0 (b) for some selected values of n with $\mu_0/\mu^* = 1/8$ are shown in **Figure 9** [12]. To create the same contact region and the

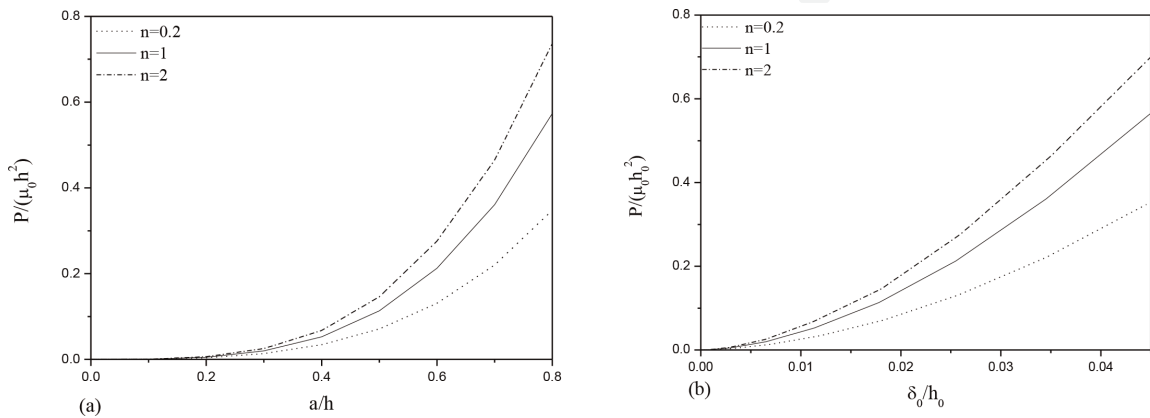


Figure 9. Relations of P vs. a (a) and P vs. δ_0 (b) for selected values of n with $R/h = 10$.

same maximum indentation depth δ_0 (b), the larger applied normal load is needed for larger values of n .

Thirdly, the effect of the variation of Poisson's ratio on the frictionless contact problem is considered by using piece wise exponential multi-layered model. The shear modulus of FGM coating varies as power law form according to Eq. (35). Poisson's ratio of FGM coating is assumed to vary as the linear function along the thickness as follows

$$v_j = v_1 + \frac{j-1}{N-1}(v^* - v_1), j = 1, 2, \dots, N \tag{36}$$

where v_1 and v^* are Poisson's ratio for the first layer and homogeneous half-space. v_j denotes Poisson's ratio in layer j . The contact pressure (a) and the relations of P vs. a (b) for the different variation forms of Poisson's ratio when $v_1 = 1/3$ and $\mu_0/\mu^* = 1/5$ are given in **Figure 10** [14]. It is assumed that Poisson's ratio for the FGM coating-substrate structure varies from $1/3$ to 0.1 and varies from $1/3$ to 0.5 according to Eq. (36). The results show that the variation of Poisson's ratio along the thickness has no significant impact on the contact pressure and the relation of force contact region in axisymmetric contact problem when the Poisson's ratio at the upper surface of coating is fixed. **Figure 11** presented the effect of value of Poisson's ratio on the contact pressure (a) and the relation of P vs. a (b) when Poisson's ratio in the coating-substrate structure is a constant ($v_j = v$) as shown in [14]. We can observe that the value of Poisson's ratio has a significant effect on the contact

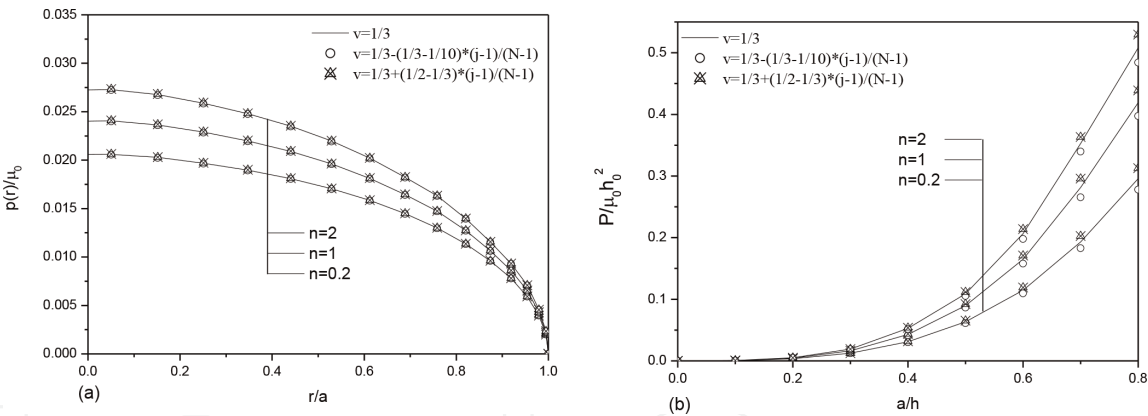


Figure 10.
The contact pressure (a) and the relations of P vs. a (b) for the different variation form of the Poisson's ratio with $v_1 = 1/3$ and $\mu_0/\mu^* = 1/5$.

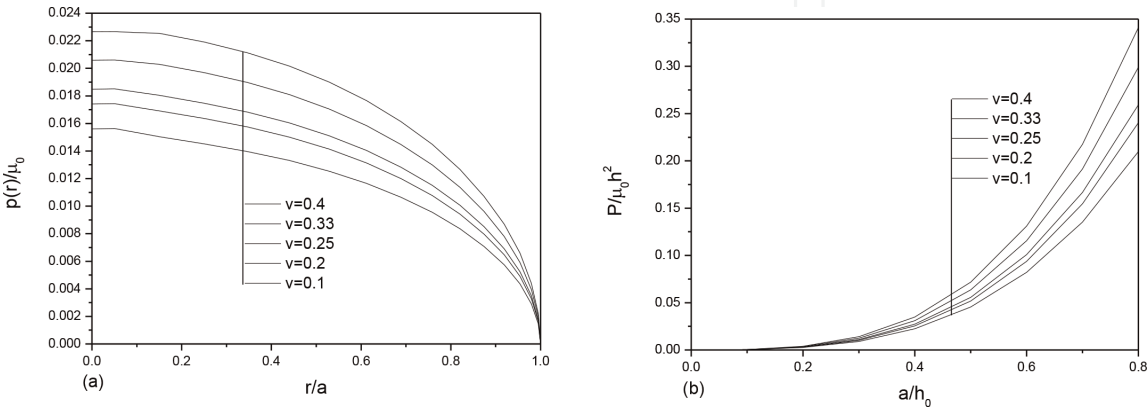
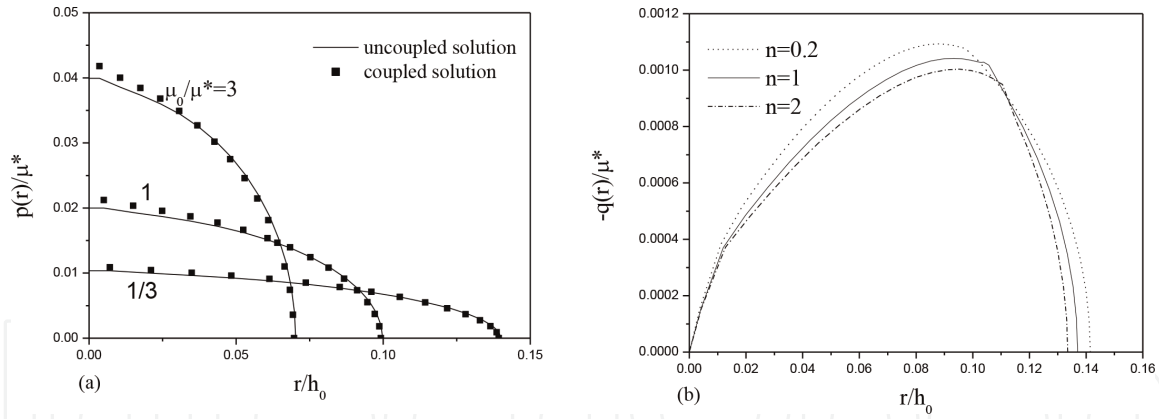


Figure 11.
The effect of the value of Poisson's ratio on the contact pressure (a) and on the relation of P vs. a (b) with $\mu_0/\mu^* = 1/5$ while $n = 0.2$.

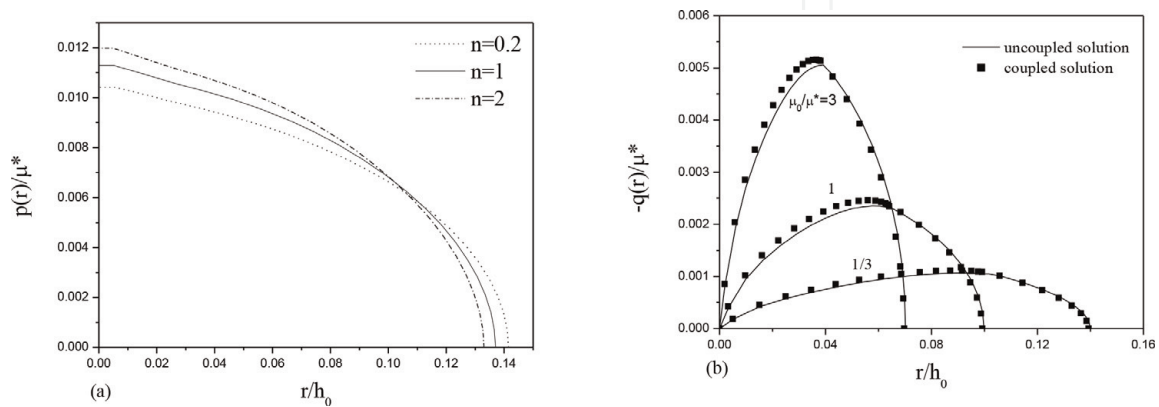

Figure 12.

Contact traction distributions for selected values of the shear modulus ratio μ_0/μ^* with $P/\mu^*h_2^0 = 4 \times 10^{-4}$ and $f = 0.16$: (a) $p(r)$ and (b) $q(r)$.

pressure. While the values of v obviously increase, the contact pressure is observed. The results also show that the larger applied normal load is needed to create the same contact region and the same maximum indentation depth δ_0 for larger values of v .

Finally, the axisymmetric contact problem of a functionally graded coated half-space is indented by a rigid spherical punch in the case of the partial slip. The linear multi-layered model is used to solve the problem.

The normal contact traction and radial tangential traction for some selected values of the shear modulus ratio μ_0/μ^* with $P/\mu^*h_2^0 = 4 \times 10^{-4}$ and $f = 0.16$ are shown in **Figure 12** [14]. The solid lines correspond to the uncoupled solution, and the scatter symbols correspond to the coupled solution. We can observe that consideration of the coupling between the normal and tangential tractions may result in the increase of the peak contact tractions but slight decrease of the contact tractions near the edges of the contact region for a given shear modulus ratio μ_0/μ^* . With the increase of μ_0/μ^* , the peak normal and tangential contact tractions increase. **Figure 12b** also shows that the stick region and the contact radius decrease with the increase of μ_0/μ^* . This behavior provides a way for us to change the distribution of the contact pressure by adjusting the stiffness of the coating surface. **Figure 13** presents the effects of n on the contact traction distributions with $P/\mu^*h_2^0 = 4 \times 10^{-4}$ and $f = 0.16$ [14]. With the increase of n , the peak normal traction (**Figure 13a**) increases, and the peak tangential traction (**Figure 13b**) decreases. This behavior provides a way for us to change the distribution of the


Figure 13.

Contact traction distributions for selected values of n with $P/\mu^*h_2^0 = 4 \times 10^{-4}$ and $f = 0.16$: (a) $p(r)$ and (b) $q(r)$.

contact traction by adjusting the gradient of the coating while remaining the shear modulus of the coating surface unchanged.

6. Conclusions

In this chapter, we introduced the axisymmetric indentation response for FGM coating under frictionless and partial slip condition by using the three types of computational models. The exponential function model can solve the axisymmetric contact problem for FGM coating whose elastic modulus continuously varies, but it cannot simulate FGM with arbitrarily varying properties. The linear multi-layered model allows arbitrarily the variation of the material properties of FGM, but it requires Poisson's ratio which is 1/3. The Piece wise exponential multi-layered model can simulate functionally graded coating with arbitrarily varying material modulus with no limit to Poisson's ratio, but numbers of sub-layers are larger. In practice, the computational model is chosen according to properties of the problem. Hankel integral transformation technology and transfer matrix method are used to solve the axisymmetric contact problem of FGM coating based on the cylindrical coordinate system. The results show that the contact behavior can be improved by adjusting the gradient of FGM coating. The present investigation will be expected to provide a guidance for design considerations and applications of FGM coating.

Acknowledgements


The support from the National Natural Science Foundation of China under Grant Nos. 11662011 and 11811530067 are gratefully acknowledged.

Author details

Tie-Jun Liu
Department of Mechanics, Inner Mongolia University of Technology, Hohhot,
China

*Address all correspondence to: liutiejun6204@163.com

IntechOpen

© 2019 The Author(s). Licensee IntechOpen. This chapter is distributed under the terms of the Creative Commons Attribution License (<http://creativecommons.org/licenses/by/3.0>), which permits unrestricted use, distribution, and reproduction in any medium, provided the original work is properly cited. 

References

- [1] Yamanoushi M, Koizumi M, Hirai T, Shiota I, editors. *Proceedings of the First International Symposium on Functionally Graded Materials*. Sendai, Japan; 1980
- [2] Suresh S. Graded materials for resistance to contact deformation and damage. *Science*. 2001;**292**:2447-2451
- [3] Giannakopoulos AE, Suresh S. Indentation of solids with gradients in elastic properties: Part I. Point force solution. *International Journal of Solids and Structures*. 1997;**34**:2357-2392
- [4] Giannakopoulos AE, Suresh S. Indentation of solids with gradients in elastic properties: Part II. Axisymmetric indenters. *International Journal of Solids and Structures*. 1997;**34**:2392-2428
- [5] Guler MA, Erdagon F. Contact mechanics of graded coatings. *International Journal of Solids and Structures*. 2004;**41**:3865-3889
- [6] Guler MA, Erdagon F. Contact mechanics of two deformable elastic solids with graded coatings. *Mechanics of Materials*. Cambridge, UK: 2006;**38**: 633-647
- [7] Liu TJ, Wang YS. Axisymmetric frictionless contact problem of a functionally graded coating with exponentially varying modulus. *Acta Mechanica*. 2008;**199**:151-165
- [8] Liu TJ, Xing YM. The axisymmetric contact problem of a coating/substrate system with a graded interfacial layer under a rigid spherical punch. *Mathematics and Mechanics of Solids*. 2016;**21**:383-399
- [9] Jeon SP, Tanigawa Y, Hata T. Axisymmetric problem of a nonhomogeneous elastic layer. *Archive of Applied Mechanics*. 1998;**68**:20-29
- [10] Ke LL, Wang YS. Two-dimensional contact mechanics of functionally graded materials with arbitrary spatial variations of material properties. *International Journal of Solids and Structures*. 2006;**4**:5779-5798
- [11] Ke LL, Wang YS. Two-dimensional sliding frictional contact of functionally graded materials. *European Journal of Mechanics - A/Solids*. 2007;**26**:171-188
- [12] Liu TJ, Wang YS, Ch Z. Axisymmetric contact problem of functionally graded materials. *Archive of Applied Mechanics*. 2008;**78**:267-282
- [13] Liu TJ, Wang YS, Xing YM. The axisymmetric partial slip contact problem of a graded coating. *Meccanica*. 2012;**47**:1673-1693
- [14] Liu TJ, Xing YM. Analysis of graded coatings for resistance to contact deformation and damage based on a new multi-layer model. *International Journal of Mechanical Sciences*. 2014;**81**: 158-164
- [15] Liu TJ, Li PX. Two-dimensional adhesion mechanics of a graded coated substrate under a rigid cylindrical punch based on a PWEML model. *Applied Mathematical Modelling*. 2019; **69**:1-14
- [16] Hertz H. *On the Contact of Elastic Solids*. Miscellaneous Papers by H. Hertz. London, UK: Macmillan; 1882
- [17] Johnson KL. *Contact Mechanics*. UK: Cambridge University Press; 1985
- [18] Spence DA. The hertz contact problem with finite friction. *Journal of Elasticity*. 1975;**5**:297-319
- [19] Ke LL, Wang YS. Fretting contact of functionally graded coated half-space with finite friction—Part I—Normal

loading. *Journal of Strain Analysis for Engineering Design*. 2007;**42**:293-304

[20] Spence DA. Self-similar solutions to adhesive contact problems with incremental loading. *Proceedings of the Royal Society of London. Series A: Mathematical and Physical Sciences*. 1968;**305**:55-80

[21] Goodman LE. Contact stress analysis of normally loaded rough spheres. *Journal of Applied Mechanics*. 1962;**29**:515-522

[22] Mossakovski VI. Compression of elastic bodies under condition of adhesion (axisymmetric case). *Szhatie uprugikh tel v usloviakh stsepleniia (Osesimmetbichnyi sluchai): PMM. Journal of Applied Mathematics and Mechanics*. 1963;**27**:418-427

[23] Norwell D, Hills DA, Sackfield A. Contact of dissimilar elastic cylinders under normal and tangential loading. *Journal of the Mechanics and Physics of Solids*. 1988;**36**:59-75

[24] Civelek MB. The axisymmetric contact problem for an elastic layer on a frictionless half-space [thesis]. Mechanical Engineering Department Lehigh University; 1972